29th International Cosmic Ray Conference Pune (2005) **00**, 101–104

Efficient Cosmic Ray Ion Production in Young Supernova Remnants

Donald C. Ellison[a] and Gamil Cassam-Chenaï[b]
(a) Physics Dept., North Carolina State Univ., Raleigh, NC 27695-8202, U.S.A.
(b) Department of Physics and Astronomy, Rutgers University, 136 Frelinghuysen Rd, Piscataway NJ 08854-8019, U.S.A.
Presenter: Don Ellison (don_ellison@ncsu.edu), usa-ellison-D-abs1-og22-oral

The strong shocks in young supernova remnants (SNRs) should accelerate cosmic rays (CRs) and no doubt exists that relativistic electrons are produced in SNRs. However, direct evidence that SNRs produce CR nuclei depends on seeing an unambiguous pion-decay feature and this has not yet been obtained. Nevertheless, the lack of an observed pion-decay feature does not necessarily mean that CR ions are not abundantly produced since ions do not radiate efficiently. If CR ions are produced efficiently by diffusive shock acceleration (DSA), their presence will modify the hydrodynamics of the SNR and produce morphological effects which can be clearly seen in radiation produced by electrons.

1. Introduction

Particle acceleration influences the SNR evolution because the production of CRs changes the effective equation of state of the shocked gas. Relativistic particles produce less pressure for a given energy density than do nonrelativistic ones and high energy particles can escape from the shock and carry away energy and pressure. The softer effective equation of state means that compression ratios well in excess of four can be produced in non-radiative, collisionless shocks (e.g., [10]). An important morphological aspect of this CR-hydro coupling is that the ratio of the forward shock radius, $R_{\rm FS}$, to the radius of the contact discontinuity, $R_{\rm CD}$, may be much less than in the test-particle case (e.g., [4][9]). If, as is generally believed, shocks put far more energy into accelerated ions than electrons, it is the efficient production of cosmic ray *ions* that reduces $R_{\rm FS}/R_{\rm CD}$ from test-particle values. Therefore, measuring $R_{\rm FS}/R_{\rm CD}$ with modern X-ray telescopes may reveal the presence of these otherwise unseen relativistic ions.

2. Model and Results

Full details of the model we use here are given in [8] and references therein. Briefly, we calculate the hydrodynamic evolution of a SNR coupled to efficient DSA. The diffusive shock acceleration process is modeled with the algebraic model of [2] and [7] where the injection efficiency is parameterized and the superthermal spectrum, $f(p)$, is a broken power law, $f_{\rm PL}(p)$, with an exponential turnover at high momenta, $f(p) \propto f_{\rm PL}(p)\exp\left(-p/p_{\rm max}\right)$. The algebraic model solves the nonlinear DSA problem at each time step of the hydro simulation given the shock speed, shock radius, ambient density and temperature, and ambient magnetic field determined in the simulation. With the accelerated distribution, an effective ratio of specific heats is calculated and used in the hydrodynamic equations, completing the coupling between the two.

The injection parameter, $\eta_{\rm inj}$, is the fraction of total protons injected into the DSA process and values $\eta_{\rm inj} \gtrsim 10^{-4}$ typically yield efficient particle acceleration rates where 10% to 99% of the available energy flux goes into relativistic protons.

As the forward shock (FS) overtakes fresh ambient medium material, the shock accelerates these particles and produces a nonthermal distribution.[1] Once the particle distribution is produced in a shell of material at the shock, it is assumed to remain in that shell as the shell convects and evolves behind the shock. During the evolution, particles experience adiabatic and synchrotron losses and in calculating the synchrotron emission and losses, we evolve the magnetic field as described, for example, in [13].

[1] We ignore pre-existing CRs and acceleration at the reverse shock and accelerate only thermal particles overtaken by the FS.

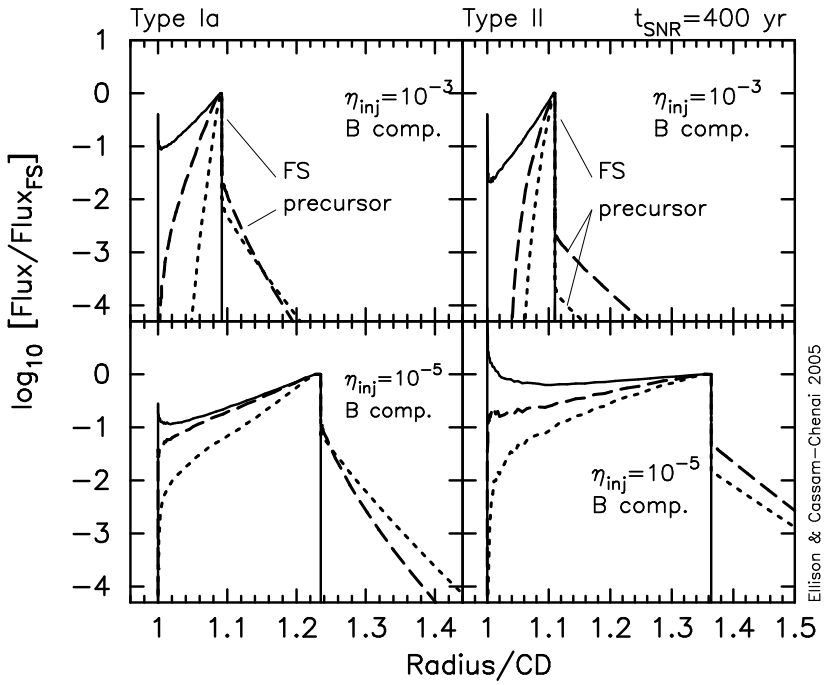

Figure 1. Radial synchrotron emission in three energy bands for two shock injection efficiencies, $\eta_{\rm inj}$. The left two panels use typical type Ia parameters where the right two panels use type II parameters (for a complete list of parameters, see [8]). In all panels, the solid curve is radio (1–1.4 GHz), the dashed curve is low energy X-rays (0.1–1 keV), and the dotted curve is high energy X-rays (1–10 keV). The flux of each band is normalized to its value at the FS. See [8] for full details.

In Fig. 1 we plot the synchrotron emission as a function of radius for one radio (1-1.4 GHz; solid curves) and two X-ray bands (0.1-1 keV dashed curves; 1-10 keV dotted curves). The two left-hand panels show results with strong CR production ($\eta_{\rm inj} = 10^{-3}$) and test-particle production ($\eta_{\rm inj} = 10^{-5}$) using typical type Ia parameters. The two right-hand panels use typical type II parameters. We note: (i) In the interaction region between the contact discontinuity and the forward shock, the X-ray synchrotron falls off more rapidly than the radio emission due to strong synchrotron losses. (ii) With efficient DSA (top panels), the X-ray fall-off is extremely rapid and the X-ray emission can appear as an extremely thin sheet at the FS. (iii) The precursor outside of the FS drops sharply due to the compressed field, making the X-ray precursor faint and difficult to detect compared to the emission at the FS. (iv) Comparing the $\eta_{\rm inj} = 10^{-3}$ panels against the $\eta_{\rm inj} = 10^{-5}$ panels shows that the distance between the CD and the FS is nearly a factor of two greater in the test-particle case than with efficient DSA. Since the limit of the shocked ejecta gives an idea of the position of the CD, $R_{\rm FS}/R_{\rm CD}$ is measurable in several young SNRs with *Chandra* and *XMM-Newton*, making this morphological difference a powerful diagnostic for efficient DSA.

In Fig. 2 we show line-of-sight (LOS) projections for the type Ia examples of Fig. 1 plotted as a fraction of the FS radius. Note that in the LOS projections the radio and X-ray peaks are offset at the FS: with or without efficient DSA, the radio peak (solid curve) occurs inside the X-ray peaks. Behavior such as this is observed in several SNRs including G347 [11], Kepler [6], Tycho [5], and Cas A [12]. Note also that because of projection effects, the maximum emission occurs inside of the FS.

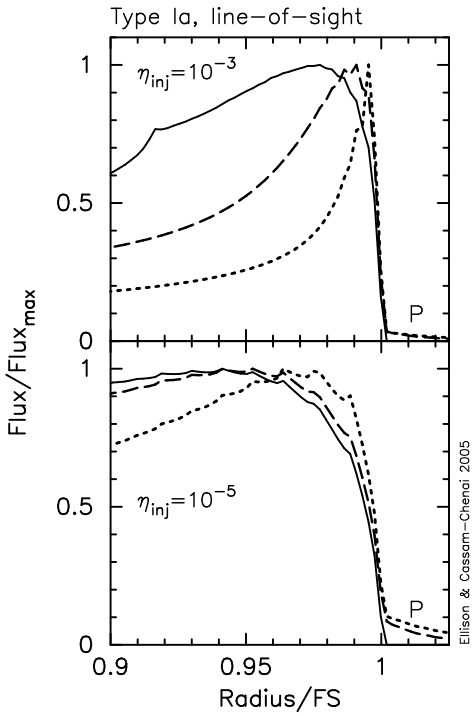

Figure 2. Line-of-sight projections for the radial distributions shown in Fig. 1 for type Ia normalized to the forward shock radius. As in Fig. 1, the solid curve is radio (1–1.4 GHz), the dashed curve is low energy X-rays (0.1–1 keV), and the dotted curve is high energy X-rays (1–10 keV). Note that the radio emission (solid curves) peaks well within the X-ray emission.

In Fig. 3 we compare our type Ia prototype model with $\eta_{\rm inj} = 10^{-3}$ to SN 1006 observations represented with dashed lines which roughly span the maximum and minimum scale heights determined by [1] (see their Table 4). As emphasized by [3], the shortest scale heights occur inside the forward shock and are produced by projection effects when B is compressed and there is a sharp drop in emissivity behind the shock. The actual upstream precursor (indicated with a "P" in Fig. 3) has a much longer scale height as expected from TeV electrons but is not easily discernable with *Chandra* against background emission. Our efficient acceleration model fits the data quite well, but a test-particle model (not shown), clearly does not. Our results, in agreement with those of [3], provide evidence for highly compressed magnetic fields and efficient DSA.

3. Discussion and Conclusions

An important signature of efficient CR ion production is a large reduction in the ratio of the radius of the forward shock to the radius of the contact discontinuity, $R_{\rm FS}/R_{\rm CD}$, caused by compression ratios $\gg 4$. This effect may explain observations of $R_{\rm FS}/R_{\rm CD} \sim 1$ in Tycho's and Kepler's SNRs. Type II SNe with pre-SN winds may experience efficient DSA yet still show large $R_{\rm FS}/R_{\rm CD} \sim$ 1.3–1.4, consistent with observations of Cas A and 1E0102.2-7219. Another sign of efficient DSA is the presence of short scale heights seen in nonthermal X-ray emission. Short scale heights are predicted because the shock will strongly compress the downstream magnetic field and synchrotron losses will lower the emissivity immediately behind the FS. Also, projection effects should result in the distinct separation of the radio and X-ray peaks.

The short scale heights seen in SN 1006 [1], are most naturally explained as sharply peaked emission behind

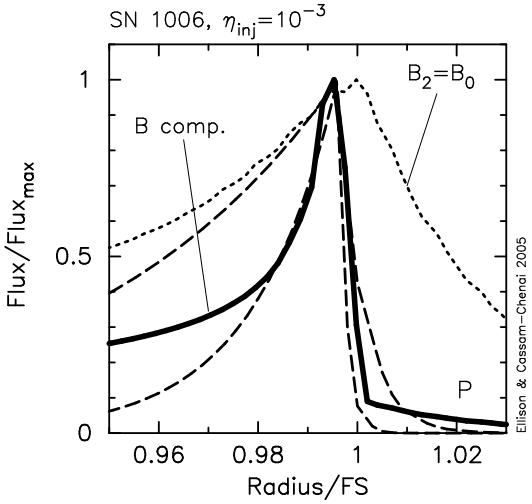

Figure 3. Comparison of X-ray LOS profiles from the CR-Hydro model with *Chandra* observations of SN 1006. The dashed curves roughly span the maximum and minimum scale heights determined by [1] where they assumed exponential profiles. Using their Table 4, we set the maximum (minimum) upstream scale height to be 3 (1) arcsec, and the downstream maximum (minimum) scale height to be 30 (10) arcsec (the radius of SN 1006 is about 0.25°). The solid curve is the X-ray emission in the 1.2–2 keV band using our compressed B model and for comparison, we show (dotted curve) the 1.2–2 keV band without compressing the field. We have positioned the peaks of the dashed curves to match the solid curve.

the FS seen in projection (e.g., [3]). The actual upstream precursor has a long scale length, as expected for TeV electrons, but is weak enough to avoid detection. Supernova remnant SN 1006 seems a clear case where the efficient production of CR ions is taking place, but remnants such as Tycho's and Kepler's, with $R_{\rm FS}/R_{\rm CD} \sim 1$, are also likely candidates.

Acknowledgements: D.C.E. wishes to acknowledge support from a NASA grant (ATP02-0042-0006).

References

[1] Bamba, A., Yamazaki, R., Ueno, M. & Koyama, K. 2003, ApJ, 589, 827
[2] Berezhko, E.G. & Ellison, D.C. 1999, ApJ, 526, 385
[3] Berezhko, E. G., Ksenofontov, L. T. & Völk, H. J. 2003, A&A, 412, L11
[4] Decourchelle, A., Ellison, D.C. & Ballet, J. 2000, ApJ, 543, L57
[5] Decourchelle, A. at al. 2001, A&A, 365, L218
[6] DeLaney, T. et al. 2002, ApJ, 580, 914
[7] Ellison, D.C., Berezhko, E.G. & Baring, M.G. 2000, ApJ, 540, 292
[8] Ellison, D.C. & Cassam-Chenaï, G. 2005, ApJ, in press
[9] Ellison, D.C., Decourchelle, A. & Ballet, J. 2004, A&A, 413, 189
[10] Jones, F.C., & Ellison, D.C. 1991, Space Sci. Rev., 58, 259
[11] Lazendic, J. S. et al. 2004, ApJ, 602, 271
[12] Long, K.S. et al. 2003, ApJ, 586, 1162
[13] Reynolds, S.P. 1998, ApJ, 493, 375